Journal of Operation and Automation in Power Engineering
Vol. 4, No. 1, Winter & Spring 2016, Pages: 42-53
http://joape.uma.ac.ir

Multi-Stage DC-AC Converter Based on New DC-DC Converter for Energy Conversion

E. Salary, M. R. Banaei*, A. Ajami
Department of Electrical Engineering, Azarbaijan Shahid Madani University, Tabriz, Iran

ABSTRACT
This paper proposes a multi-stage power generation system suitable for renewable energy sources, which is composed of a DC-DC power converter and a three-phase inverter. The DC-DC power converter is a boost converter to convert the output voltage of the DC source into two voltage sources. The DC-DC converter has two switches operates like a continuous conduction mode. The input current of DC-DC converter has low ripple and voltage of semiconductors is lower than the output voltage. The three-phase inverter is a T-type inverter. This inverter requires two balance DC sources. The inverter part converts the two output voltage sources of DC-DC power converter into a five-level line to line AC voltage. Simulation results are given to show the overall system performance, including AC voltage generation. A prototype is developed and tested to verify the performance of the converter.

KEYWORDS: Renewable energy, Multi-stage inverter, DC-DC converter, Multi-level inverter.

1. INTRODUCTION

Distributed generation (DG) systems as local power sources have great potential to contribute toward energy sustainability, energy efficiency and supply reliability. In the electrical power system, the most important driving forces for the proliferation of DGs are [1-3]:

- Liberalized electricity market
- environmental concerns with greenhouse gas emissions
- energy efficiency
- diversified energy sources constitute
- peak shaving capability

The power conversion interface is important to load or grid-connected DG power generation systems. Some DGs such as Fuel cell (FC) and photovoltaic (PV) generate DC voltage so an inverter is necessary to convert the DC power to AC power [4-6]. Since the output voltage of a PV or FC array is low, a DC-DC power converter is used in a power generation system to boost the output voltage. Variable voltage is one of the most important problems of the fuel cells. PVs are small power resources and it is essential to choose a suitable method of maximum power point tracking (MPPT). Output voltages of the PV modules are variable because of changes of temperature and sunlight irradiation. Different type of MPPT algorithms have suggested in different papers. Among the MPPT techniques, the perturbation and observation (P&O) method and incremental conductance are the most popular because of the simplicity of its control structure [3]. The PV system requires DC-DC converters with a flexible control range to obtain maximum power and increasing voltage. Input current ripple is an important feature for DC-DC converters, used in fuel cell applications. The low current ripple increases the efficiency and lifetime of the fuel cells. In multi-stage converter, inverter part generates AC voltage and injects power to the grid.

The DC-DC converter with high step-up voltage gain is widely used for energy conversion systems. Conventionally, the classic DC-DC boost converter is used for voltage step-up applications. In high step-up voltage gain this converter will be operated at a high duty ratio [7]. Some literatures have researched

Received: 3 June 2015 Revised: 9 Sep. 2015
Accepted: 12 Oct. 2015
*Corresponding author:
M. R. Banaei (m.banaei@azaruniv.edu)

the high step-up DC-DC converters that do not incur an extremely high duty ratio [8-12].

Multilevel inverter technology has appeared recently as a very important alternative in the area of the power system. In theory, multilevel inverters should be designed with higher voltage levels in order to improve the conversion efficiency and to reduce harmonic content and electromagnetic interference. This technology can be used in energy conversion. They can generate output voltages with extremely low distortion and lower dv/dt [13,14]. The different topologies presented in the literature as multilevel converters. The most popular multilevel converters are the diode-clamped, flying capacitor and cascaded H-bridge structures. In recent years, novel topologies of multilevel inverters using a reduced number of switches and gate driver circuits have presented [15-17]. Unfortunately, multilevel inverters have some disadvantages. One particular disadvantage is the great number of power semiconductor switches needed. Although low voltage rate switches can be utilized in a multilevel inverter, each switch requires a related gate driver circuit. This may cause the overall system to be more expensive and complex. So, in practical implementation, reducing the number of switches and gate driver circuits is very important.

It seems that using of multilevel inverter with high number of voltage levels and switches is not commodious in low voltage application. The multilevel inverter with a low number of levels needs a less number of switches and can be suitable for low voltage application. In Ref. [18], a five-level inverter is developed and applied for injecting the real power of the renewable power into the grid to reduce the switching power loss, harmonic distortion, and electromagnetic interference caused by the switching operation of power electronic devices. This topology uses six switches and two diodes in one phase. In Ref. [19] the hybrid seven-level cascaded active neutral-point-clamped (ANPC) based multilevel converter is presented. The converter topology is the cascaded connection of a three-level ANPC converter and an H-bridge per phase. This topology uses ten switches in one phase. In Ref. [20], a seven-level inverter topology, configured by a level generation part and a polarity generation part, is proposed. There, only power electronic switches of the level generation part switch in high frequency, but ten power electronic switches and three DC capacitors are used. The T-type multilevel converter is one type of multilevel inverters that is introduced in Ref. [21]. This inverter is suitable for using grid distribution voltage (400 or 380 V). This converter uses two DC-link capacitor and nine switches.

In this paper, one DC-AC converter based T-type multilevel inverter is presented. The proposed converter has two parts: DC-DC converters and T-type multilevel inverter. In T-type, the conventional six switches inverter is converted to a multilevel inverter topology that requires only nine active switches. A new type of DC-DC converter is used to provide DC-link voltages for multilevel inverter. The main advantages of DC-DC converter are low input current ripple and high voltage gain. In this letter, the operating principle of the developed system is described, and a prototype of inverter is constructed for verifying the effectiveness of the topology. A case study about fuel cell power generation is studied.

2. MULTI-STAGE DC-AC CONVERTER

Figure 1 shows the configuration of the proposed multi-stage system. The proposed system is composed of a DC voltage source array, a DC-DC power converter and T-type multilevel inverter. The DC voltage source is connected to the DC-DC converter that is a boost converter. The boost DC-DC converter converts the output power of the DC voltage into two voltage sources, which supply the inverter.

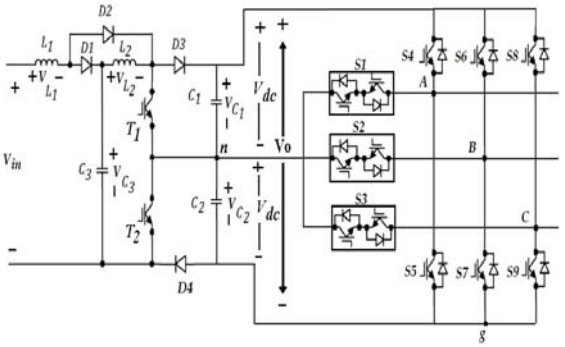

Fig. 1. Configuration of the proposed multi-stage system.

The T-type multilevel inverter is composed of

three bidirectional switches and a conventional six switches power converter, connected in cascade. As can be seen, T-type multilevel inverter contains only nine switches, so, the power circuit is simplified.

2.1. DC-DC converter

In a classic DC-DC boost converter, the voltage stresses on the switch and diode, which are equal to the output voltage, are high. In the proposed multi-stage converter, a step-up DC-DC converter is used, as shown in Fig. 1. Inside DC-DC converter, the semiconductor device voltage rating is only half of the output voltage. Special modulation technique, offers lower input current ripple and output voltage ripple. The peak inverse voltage of switches and diodes is half of output voltage.

In order to simplify the circuit analysis of the converter, all components are assumed ideal. The voltage of capacitors is equal. To operation analysis of DC-DC converter, it is assumed that converter has one resistive load.

$$V_{C1} = V_{C2} = V_{dc} \tag{1}$$

The output voltage is equal to sum of voltage of output capacitors.

$$V_O = V_{C1} + V_{C2} = 2V_{dc} \tag{2}$$

The proposed converter operates in continuous conduction mode (CCM) and discontinuous conduction mode (DCM). Here, CCM is analyzed and discussed.

Based on the aforementioned assumptions, there are three operating modes discussed in one switching period under CCM operation.

Figure 2 shows the topology stages of the proposed converter. The operating modes are described as follows.

Mode 1: Fig. 2(a) shows mode 1 equivalent circuit. During this mode T_1 and T_2 are turned on. The DC-source energy is transferred to L_1 and L_2 is charged by C_3, so currents of inductors are increased. In this mode D_2 is turned on and D_1, D_3 and D_4 are turned off. Energy of output capacitors are given to load.

$$V_{L1} = V_{in} \tag{3}$$

$$V_{L2} = V_{C3} \tag{4}$$

Duration of mode 1 is equal as:

$$t_1 = DT = \frac{D}{f_D} \tag{5}$$

where, D, T and f_D are the duty cycle switching period and switching frequency, respectively.

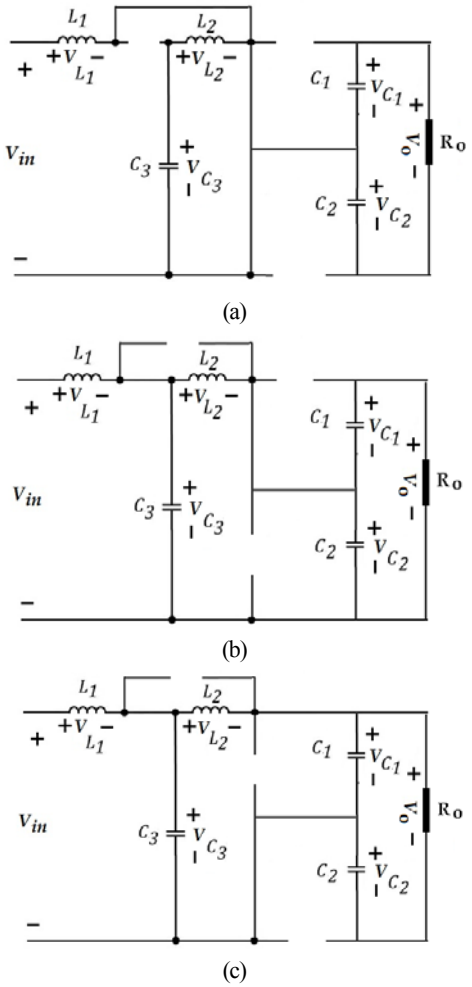

Fig. 2. Topological stages of the proposed converter (a) mode 1 (b) mode 2 and (c) mode 3.

Mode 2: T_1 is turned on and T_2 is turned off. The energy is pumped to C_2 and C_3 while the energy of C_1 is given to load. The currents of inductors decrease. Fig. 2(b) shows mode 2 equivalent circuit. During mode 2, the voltage across the inductors is:

$$V_{L1} = V_{in} - V_{C3} \tag{6}$$

$$V_{L2} = V_{C3} - V_{C2} = V_{C3} - \frac{V_O}{2} \tag{7}$$

Duration of mode 2 is equal as:

$$t_2 = (\frac{1-D}{2})T \tag{8}$$

Mode 3: T_1 is turned off and T_2 is turned on. The energy is pumped to C_1 through T_2, and D_3, so, the

currents of inductors are decreased. Fig. 2(c) shows mode 3 equivalent circuit. During mode 3, the voltage across the inductor is:

$$V_{L1} = V_{in} - V_{C3} \tag{9}$$

$$V_{L2} = V_{C3} - V_{C1} = V_{C3} - V_O/2 \tag{10}$$

Duration of mode 3 is equal as:

$$t_3 = ((1-D)/2)T \tag{11}$$

The inductor average voltage and capacitor average current over one cycle is zero [11].

$$\overline{V_{L1}} = 0 = D.V_{in} + \frac{2(1-D)}{2}(V_{in} - V_{C3}) \Rightarrow V_{C3} = \frac{V_{in}}{(1-D)} \tag{12}$$

$$\overline{V_{L2}} = 0 = D.V_{C3} + \frac{2(1-D)}{2}(V_{C3} - \frac{V_O}{2}) \Rightarrow V_O = \frac{2V_{C3}}{(1-D)} \tag{13}$$

$$\overline{i_{C3}} = 0 = -D.I_{L2} + (1-D)(I_{L1} - I_{L2}) \Rightarrow I_{L2} = \frac{I_{L1}}{(1-D)} \tag{14}$$

Substituting Eq. (12) into Eq. (13) yields the voltage conversion ratio of the proposed converter,

$$V_O = \frac{2V_{in}}{(1-D)^2} \tag{15}$$

Figure 3 shows modulation waveforms and gate signals in one period. The modulation technique is expressed as follows:

If (-D ≤ triangular ≤ D) then T_1: on, T_2: on

If (triangular > D) then T_1: on, T_2: off

If (triangular < -D) then T_1: off, T_2: on

Figure 4 shows the signal gates, voltage and current of input inductor (L_1). The charge and discharge of L_2 are the same as L_1. The frequency of inductor current is doubling of switching frequency. Based on Eq. (15), the input current I_{L1} can be expressed as:

$$I_{L1} = \frac{2V_O}{R(1-D)^2} = \frac{2I_O}{(1-D)^2} \tag{16}$$

Where, I_O is the output current. In addition, the current ripple of i_{L1} and i_{L1} denoted by Δi_{L1} and Δi_{L2}, respectively. The current ripple of inductors can be expressed to be

$$\Delta i_{L1} = \frac{DT}{2L_1}V_{in} = \frac{D(1-D)^2T}{4L_1}V_O \tag{17}$$

$$\Delta i_{L2} = \frac{(1-D)DT}{4L_2}V_O \tag{18}$$

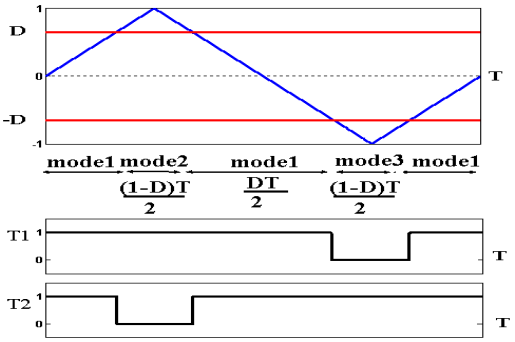

Fig. 3. Modulation waveforms and gate signals in one period.

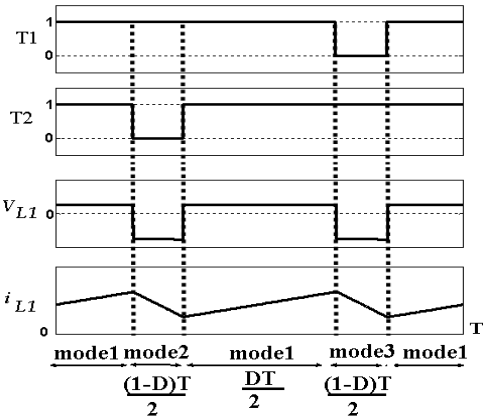

Fig. 4. The signal gates, voltage and current of input inductor (L_1).

The ripple of inductor current is half of ripple of inductor current in classic boost DC-DC converter. This is one advantage of proposed converter.

From Eqs. (15) and (16), for steady-state analysis of the boundary condition mode (BCM) we have:

$$I_{L1} = \frac{\Delta i_{L1}}{2} = \frac{D.T}{4L_1}V_{in} = \frac{2I_O}{(1-D)^2} \tag{19}$$

$$L_1 = \frac{D(1-D)^4TV_O}{16I_O} = \frac{D(1-D)^4TR_O}{16} \tag{20}$$

Where

$$R_O = V_O / I_O \tag{21}$$

The normalized magnetizing-inductor time constant is defined as Eqs. (22) and (25). BCM condition for L_1 and L_2 is shown in Fig. 5.

$$\tau_{L1} = \frac{L_1}{T.R_O} = \frac{D(1-D)^4}{16} \tag{22}$$

$$I_{L2}=\frac{2I_O}{(1-D)}=\frac{\Delta i_{L2}}{2}=\frac{DT}{4L_2}\frac{V_{in}}{(1-D)} \quad (23)$$

$$L_2=\frac{D(1-D)^2TR_O}{16} \quad (24)$$

$$\tau_{L2}=\frac{L_2}{T.R_O}=\frac{D(1-D)^2}{16} \quad (25)$$

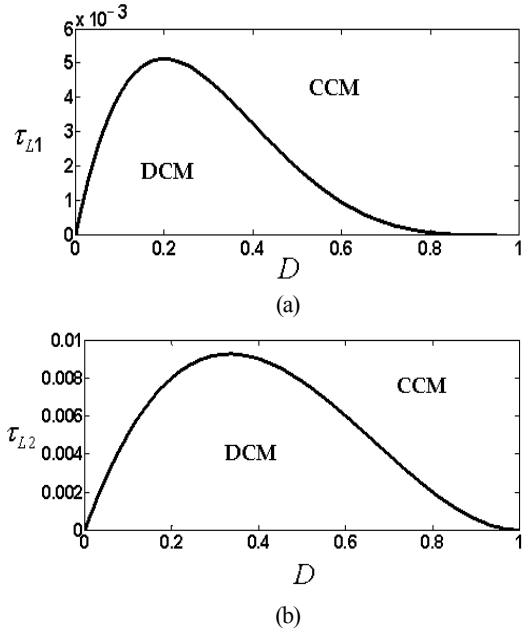

Fig. 5. BCM condition for L_1 and L_2.

During mode 1, L_2 discharges the C_3 capacitor therefore; the voltage ripple across the C_3 capacitors can be expressed as:

$$\Delta V_{C3}=\frac{DT}{2C_3}I_{L2}=\frac{DT}{(1-D)C_3}I_O \quad (26)$$

If C_1 is equal to C_2 then the voltage ripple of output capacitors is shown as Eq. (27).

$$\Delta V_{C1}=\frac{(1+D)T}{2C_1}I_O \quad (27)$$

Another important problem in power electronic converters is the ratings of switches. In other word, voltage and current ratings of the switches in a converter play important roles on the cost and realization.

The PIV on semiconductors are given as:

$$V_{T1}=V_{T2}=V_{D3}=V_{D4}=\frac{V_O}{2} \quad (28)$$

$$V_{D1}=\frac{(1-D)V_O}{2} \quad (29)$$

$$V_{D2}=DV_O/2 \quad (30)$$

If inductors are large enough, the current of inductors can be calculated as Eqs. (15) and (23) and they are constant in one period. The current of semiconductor is given as bellow based on current of inductors.

$$i_{D1}=\begin{cases}0 & DT\\ I_{L1} & (1-D)T\end{cases} \quad (31)$$

$$I_{D1}=\sqrt{(1-D)}I_{L1} \quad (32)$$

$$I_{D1av}=(1-D)I_{L1} \quad (33)$$

$$i_{D2}=\begin{cases}I_{L1} & DT\\ 0 & (1-D)T\end{cases} \quad (34)$$

$$I_{D2}=\sqrt{D}I_{L1} \quad (35)$$

$$I_{D2av}=DI_{l1} \quad (36)$$

$$i_{T1}=i_{T2}=\begin{cases}I_{L1}+I_{L2} & DT\\ I_{L2} & \frac{(1-D)T}{2}\\ 0 & \frac{(1-D)T}{2}\end{cases} \quad (37)$$

$$I_{T1}=I_{T2}=\sqrt{(I_{L1}+I_{L2})^2D+{I_{L2}}^2\frac{(1-D)}{2}} \quad (38)$$

$$I_{T1av}=I_{T2av}=(I_{L1}+I_{L2})D+I_{L2}\frac{(1-D)}{2} \quad (39)$$

$$i_{D3}=i_{D4}=\begin{cases}0 & DT\\ I_{L2} & \frac{(1-D)T}{2}\\ 0 & \frac{(1-D)T}{2}\end{cases} \quad (40)$$

$$I_{D3}=I_{D4}=I_{L2}\sqrt{(\frac{1-D}{2})} \quad (41)$$

$$I_{D3av}=I_{D4av}=I_{L2}(\frac{1-D}{2}) \quad (42)$$

Figure 6 shows the voltage gain versus the duty ratio of the proposed converter and cascaded boost converter. As it is shown in Fig. 6, the presented converter has higher voltage gain.

2.2. DC-AC converter

The T-type three-level inverter is formed by the nine main power devices. A capacitor voltage divider, formed by C_1 and C_2 provides a half supply voltage

point, node *n* in Fig. 1. The auxiliary switches, formed by the controlled bidirectional switch S1, S2 and S3, connect the center point of the left hand three-level inverter to the node *n*.

The required three voltage output levels for one phase (V_{An}) are generated as follows:

1) Zero output: The auxiliary switches S1 is on, short-circuiting the V_{An} and V_{An}=0. All other controlled switches in phase A are off.

2) Maximum positive output, V_{dc}: S4 is on, connecting the node A to V_{dc} and $V_{An}=V_{dc}$. All other controlled switches are off.

3) Maximum negative output, $-V_{dc}$: S5 is on, connecting the node A to V_{dc} and $V_{An}=-V_{dc}$. All other controlled switches are off.

In the switching strategy, in one phase at any time only one switch is on. The T-type inverter is able to generate five voltage levels in the line-to-line output voltage. The line-to-line output voltages are given as:

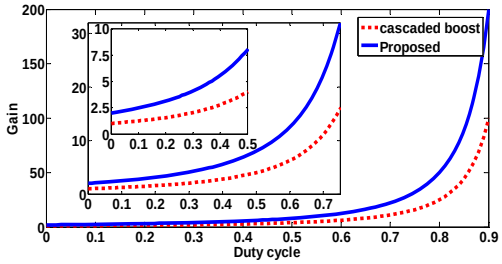

Fig. 6. The voltage gain versus the duty ratio of the proposed converter and cascaded boost converter.

$$\begin{cases} V_{AB} = V_{An} - V_{Bn} \\ V_{BC} = V_{Bn} - V_{Cn} \\ V_{CA} = V_{Cn} - V_{An} \end{cases} \quad (43)$$

Table 1 shows the on switches lookup table of five-level multilevel inverter. It is clear that switches in one phase can't be on simultaneously, because a short circuit across the voltage V_{dc}.

Since only three power electronic switches are used in the proposed inverter in one phase, the power circuit is significantly simplified. The states of the power electronic switches of the five-level inverter, as detailed previously, are summarized in Table 1. It can be seen that only one power electronic switch is switched for each switching operation.

The PIV on switches are given as:

$$V_{S1} = V_{S2} = V_{S3} = \frac{V_O}{2} \quad (44)$$

$$V_{S4} = V_{S5} = V_{S6} = V_{S7} = V_{S8} = V_O \quad (45)$$

Table 1. Lookup table of a three-phase inverter.

On Switches	V_{AB}	V_{BC}	V_{CA}
S4 S7 S8	$2V_{dc}$	$-2V_{dc}$	0
S4 S7 S3	$2V_{dc}$	$-V_{dc}$	$-V_{dc}$
S4 S7 S9	$2V_{dc}$	0	$-2V_{dc}$
S4 S2 S9	V_{dc}	V_{dc}	$-2V_{dc}$
S4 S6 S9	0	$2V_{dc}$	$-2V_{dc}$
S1 S6 S9	$-V_{dc}$	$2V_{dc}$	$-V_{dc}$
S5 S6 S9	$-2V_{dc}$	$2V_{dc}$	0
S5 S6 S3	$-2V_{dc}$	V_{dc}	V_{dc}
S5 S6 S8	$-2V_{dc}$	0	$2V_{dc}$
S5 S2 S8	$-V_{dc}$	$-V_{dc}$	$2V_{dc}$
S5 S7 S8	0	$-2V_{dc}$	$2V_{dc}$
S1 S7 S8	V_{dc}	$-2V_{dc}$	V_{dc}

Although the S1, S2 and S3 are bidirectional switches but the PIV of these switches are half of other switches. The voltage changing of switches is lower than conventional three-level inverter. The d*v*/d*t* is given as:

$$\frac{dv}{dt} = \frac{V_O}{2} \quad (46)$$

3. CASE STUDY

The DG units can be operated in stand-alone mode (independent of the grid) or at grid tied mode (connected to the grid). In both modes, DG unit feeds load or power system through an inverter. In this paper, a system shown in Fig. 7 is a case study. In the case study operation of converter in grid tied mode is discussed. In the case study, generated power by FC injects to the grid. The basic control schemes used in the DC-DC and DC-AC converters are shown in Fig. 7. The DC-DC converter control scheme consists of one loop control. The I_{in} is the measured input current and I^*_{in} is the reference current provided by

$$I^*_{in} = \frac{P^*_{FC}}{V_{in}} = \frac{P^*_{in}}{V_{in}} \quad (47)$$

where, P^*_{FC} is reference power of FC. The control loop consists of a conventional PI controller.

Regarding the DC-AC converter, it can operate in a grid tied mode. In the case of grid-connected mode, a decoupled control strategy is used.

The voltage equations in the stationary frame are:

$$e_a = E\cos(\omega t) = V_{Ao} - L_f \frac{di_a}{dt}$$
$$e_b = E\cos(\omega t - \frac{2\pi}{3}) = V_{Bo} - L_f \frac{di_b}{dt} \quad (48)$$
$$e_b = E\cos(\omega t - \frac{4\pi}{3}) = V_{Co} - L_f \frac{di_c}{dt}$$

where, E and ω are the maximum phase voltage and angular frequency of the grid, respectively. The voltage equations in the synchronous frame (dq) are given by

$$\begin{bmatrix} e_d \\ e_q \end{bmatrix} = -L_f \frac{d}{dt}\begin{bmatrix} i_d \\ i_q \end{bmatrix} - \omega L_f \begin{bmatrix} -i_q \\ i_d \end{bmatrix} + \begin{bmatrix} V_d \\ V_q \end{bmatrix} \quad (49)$$

where, e_d and i_d are the d-axis output voltage and current and e_q and i_q are the q-axis output voltage and current. The grid voltages of dq-axis are E and zero.

For a unity power factor, it is desirable that the q-axis current is zero. Then the q-axis current is controlled with the zero reference current. The active power supplied to the grid is:

$$P = \frac{3}{2}(e_d i_d + e_q i_q) = \frac{3}{2} E i_d \quad (50)$$

Since the active power is directly proportional to the d-axis current, the d-axis reference current is generated from the PI voltage controller for the DC-link voltage regulation. The conventional PI voltage controller is:

$$i_d^* = k_p(V_{dc}^* - V_{dc}) + k_i \int (V_{dc}^* - V_{dc})dt \quad (51)$$

where, V_{dc}^* and V_{dc} are the reference DC-link voltage and the DC-link voltage k_p and k_i are the proportional and integral control gains of the PI voltage controller. The following decoupling control is:

$$V_d = E - \omega L_f i_q + \Delta V_d \quad (52)$$
$$V_q = \omega L_f i_d + \Delta V_q \quad (53)$$

The output signals ΔV_d and ΔV_q of the current controllers generate transient additional voltages required to maintain the sinusoidal input currents.

$$\Delta V_d = k_{pd}(i_d^* - i_d) + k_{id} \int (i_d^* - i_d)dt \quad (54)$$
$$\Delta V_q = k_{pq}(i_q^* - i_q) + k_{iq} \int (i_q^* - i_q)dt \quad (55)$$

k_{pd} and k_{id} are proportional control gains and k_{pq} and k_{iq} are integral control gains.

3. SIMULATION RESULTS

To confirm the feasibility of the proposed converter and the analyses done above, simulation results are carried out by using MATLAB/SIMULINK software. Two parts of simulations are carried out.

In the first simulation the operation of DC-DC boost converter is studied and in the second simulation operation of the proposed converter in the case study is shown. There are several modulation strategies for inverters [21- 24].

3.1. Operation of boost DC-DC converter

Table 2 shows parameters of DC-DC converter. This converter is used to increase the 96 V input voltage to 768 V at the output. According to Eq. (15), duty cycle is 0.5. The frequency of switching is 25 kHz. $\Delta i_{in}/I_{in}$ is lower than 5% and is $\Delta v_o/V_O$ lower than 1%. Fig. 8 depicts the output voltage and current. The output voltage is 768 V.

Figure 9 shows voltage of semiconductors. Fig. 9 (a) shows voltage of switches (T_1 and T_2). The voltages of diodes are shown in Fig. 9(b).

The voltages of semiconductors are lower than output voltage. It should be noted that, the voltage stress value of the diode D_1 and D_2 is lower than other semiconductors. Fig. 10 shows the voltages and currents of inductors. The input current (I_{L1}) is shown in Fig. 10(a). The ripple of input current is 1.925 A. Fig. 11 depicts the currents of semiconductors.

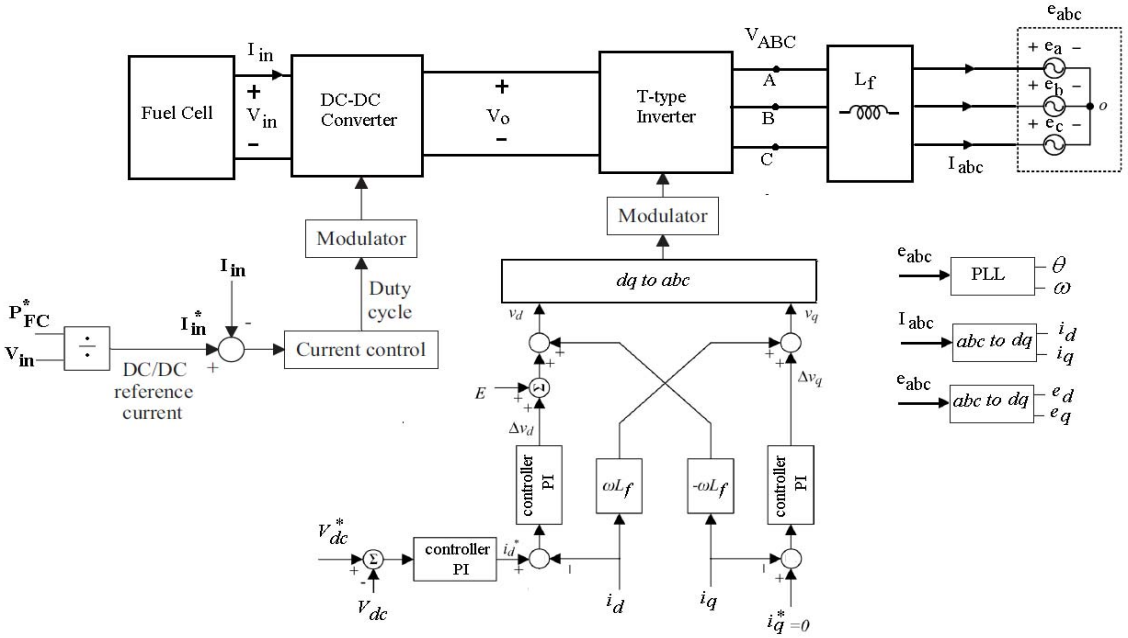

Fig. 7. Case study.

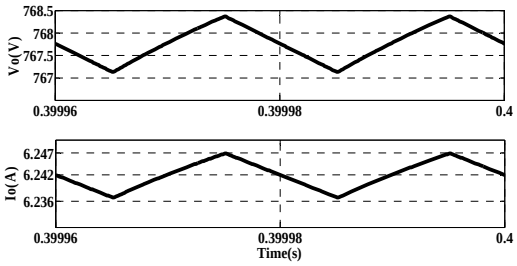

Fig. 8. Output voltage and current.

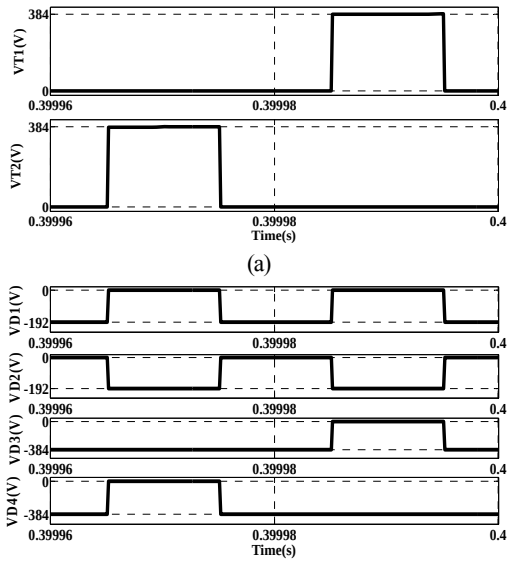

Fig. 9. Voltage of semiconductors (a) voltage of switches (T_1 and T_2) and (b) voltages of diodes.

Table 2. Parameters of DC-DC converter.

DC source	96 V
L_1, L_2	500 µH
C_1, C_2 and C_3	100 µF
Switching frequency	25000 Hz
D	0.5
Load	102 Ω

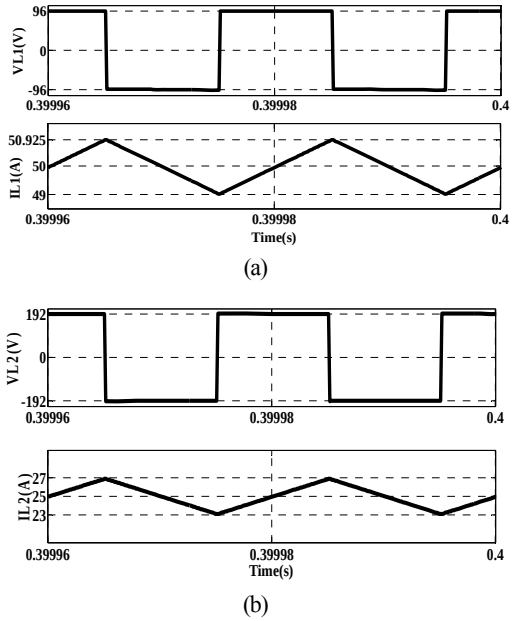

Fig. 10. Voltages and currents of inductors (a) Voltage and current of L_1 and (b) Voltage and current of L_2.

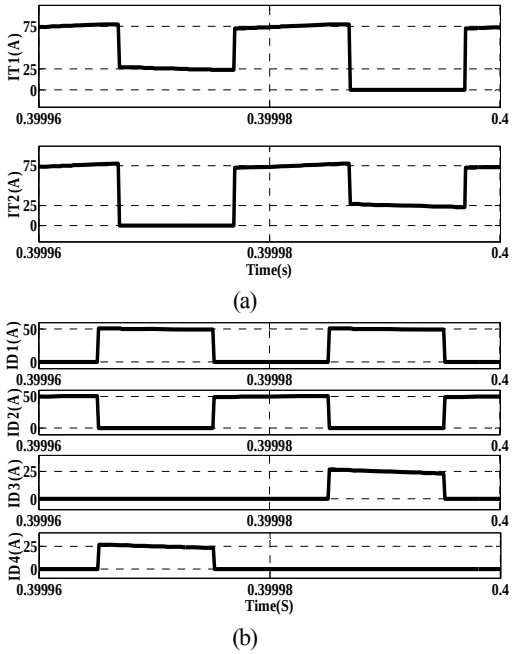

Fig. 11. Currents of semiconductors (a) currents of switches (T_1 and T_2) and (b) currents of diodes.

A low current ripple is an important factor in fuel cell applications.

3.2. Case study simulation

Table 3 shows the parameters of case study simulation. Injection of generating power from FC into the grid is the main goal of the case study. Two cells of FC are connected as series to create DC source. In the case study simulation, the generated power change in 0.4 s.

Figure 12 shows input voltage and current of DC source. The generated power by FC (P_{in}) and injected power to the grid (P) is shown in Fig. 13. The exchanged power between FC and grid is shown in Fig.13. The voltage of DC-link is shown in Fig. 14. Fig. 15 shows the line to line voltage. This voltage has five levels.

Table 3. Parameters of Case study.

Parameters	values
Fuel cell	AFC, 2.4 KW, 48 V
Voltage of DC bus(V_O)	700 V
Nominal frequency	50Hz
Grid voltage	380 V
L_f	750 μH
Inverter frequency	5000 Hz

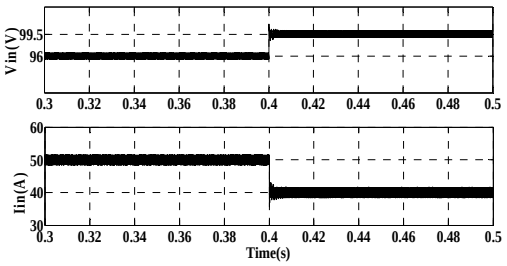

Fig. 12. Input voltage and current of source.

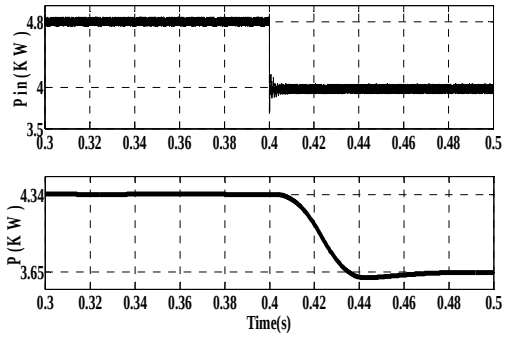

Fig. 13. The exchanged power between FC and grid.

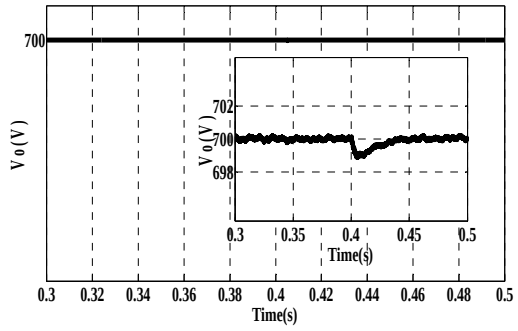

Fig. 14. Voltage of DC-link.

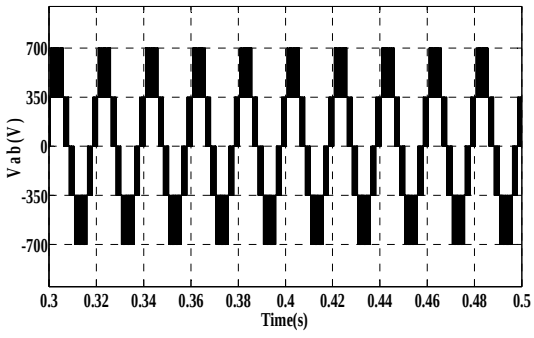

Fig. 15. line to line voltage.

4. EXPRIMENTAL RESULTS

To verify the performance of the converter, a prototype based on the DSP28335 is developed and tested. The parameters of the prototype are listed in Table 4. The DSPTMS320F28335 is used to

implement controller and the opto coupler TLP250 is used to drive switches. The fundamental switching frequency is used for inverter part. Fig. 16 shows photographs of the different parts of prototype. The DC-DC converter elements are shown in Fig. 16(a). Fig. 17 shows gate pulse of DC-DC converter. Fig. 18 shows waveforms of DC-DC converter. The input current is shown in Fig. 18(a). Fig. 18(b) shows voltage of capacitors. The dc-link voltage (output voltage of DC-DC converter) is sum of voltage of C_1 and C_2. Fig. 18(c) shows dc-link voltage. Fig. 19 shows the measured output voltage waveforms of inverter part. This is a 50Hz staircase waveform. As it can be seen, the results verify the ability of the proposed inverter in generation of desired output voltage waveform. Fig. 19(a) shows the output voltage of the phases to node n. Each phase generates a quasi-square waveform. Fig. 19(b) shows the line to line output voltage.

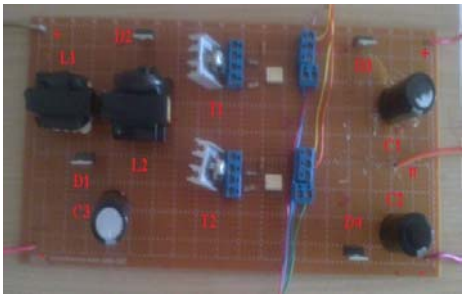

(a)

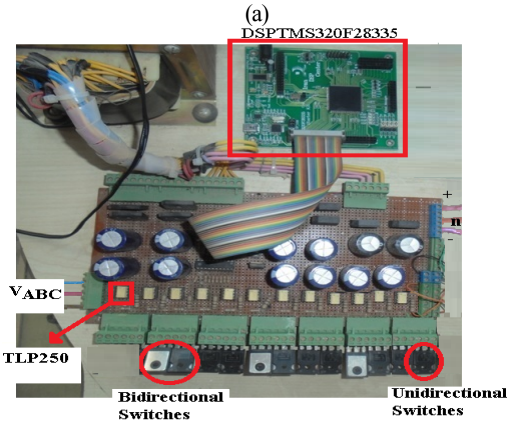

(b)

Fig. 16. Laboratory prototype of proposed converter (a) DC-DC converter and (b) DC-AC inverter.

Table 4. Parameters of experimental results.

DC source	12 V
L_1, L_2	500, 500 µH
C_1, C_2 and C_3	1000 µF
DC-DC Switching frequency	15800 Hz
D	0.5
Load	75 Ω

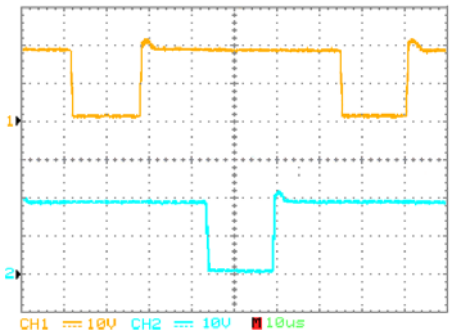

Fig. 17. Laboratory Gate pulses of DC-DC converter.

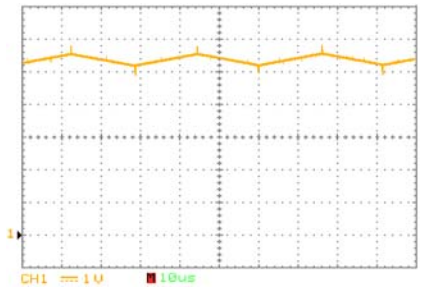

(a)

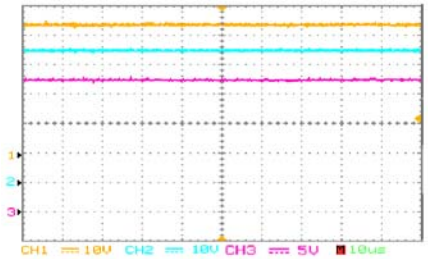

(b)

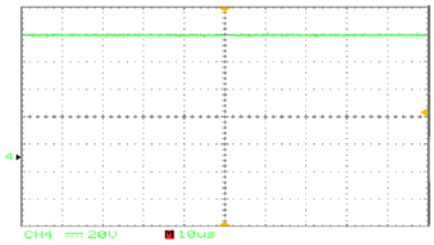

(c)

Fig. 18. Waveforms of DC-DC converter (a) input current (b) voltage of capacitors and (c) output voltage.

5. CONCLUSIONS

This paper proposes a multi-stage inverter for FC applications. The high step-up DC-DC converter is employed to provide a high voltage gain. The first stage is a boost converter that has a higher gain than the conventional boost converter to enable reducing the number of series connected FC modules. In order to investigate the performance of the converter in fuel cell systems, parameters such as voltage transfer gain and input current ripple are calculated.

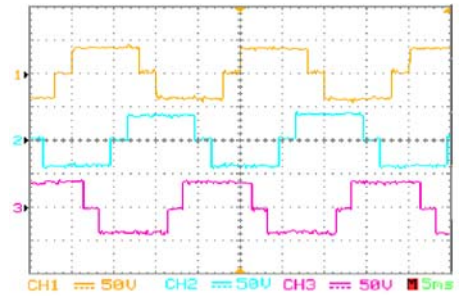

(a)

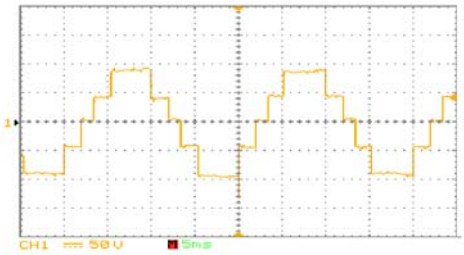

(b)

Fig. 19. Measured output voltages (a) V_{An}, V_{Bn}, V_{Cn} and (b) V_{AB}.

The simulation results demonstrate considerable increase in voltage transfer gain and reduction in input current ripple. These parameters are the most important features in fuel cell DC-DC converters. The second stage is a T-type inverter. This inverter is based on the two level inverter topology where it consists of a main inverter switches and an auxiliary three bidirectional switches. Equations of converters have been presented for DC-DC and DC-AC part. Simulation and experimental results are given to show the overall system performance.

REFERENCES

[1] M. Allahnoori, Sh. Kazemi, H. Abdi and R. Keyhani, "Reliability assessment of distribution systems in presence of microgrids considering uncertainty in generation and load demand," *Journal of Operation and Automation in Power Engineering*, vol. 2, no. 2, pp. 113- 120, 2014.

[2] K.N. Reddy and V. Agarwal, "Utility interactive hybrid distributed generation scheme with compensation feature," *IEEE Transactions on Energy Conversion*, vol. 22, no. 3, pp. 666-673, 2007.

[3] D. Sera, R. Teodorescu, J. Hantschel and M. Knoll, "Optimized maximum power point tracker for fast-changing environmental conditions," *IEEE Transactions on Industrial Electronics*, vol. 55, no. 7, pp. 2629-2637, 2008.

[4] U.S. Selamogullari, D. A. Torrey and S. Salon, "A systems approach for a stand-alone residential fuel cell power inverter design," *IEEE Transactions on Energy Conversion*, vol. 25, no. 3, pp. 741-749, 2010.

[5] Z. Zhao, M. Xu, Q. Chen, J.S Jason Lai and Y. H. Cho, "Derivation, analysis, and implementation of a boost-buck converter-based high-efficiency pv inverter," *IEEE Transactions on Power Electronics*, vol. 27, no. 3, pp.1304-1313, 2012.

[6] J.M. Shen, H.L. Jou and J.C. Wu, "Novel transformer-less grid-connected power converter with negative grounding for photovoltaic generation system," *IEEE Transactions on Power Electronics*, vol. 27, no. 4, pp.1818-1829, 2012.

[7] D.C. Lu, K.W. Cheng and Y.S. Lee, "A single-switch continuous-conduction-mode boost converter with reduced reverse-recovery and switching losses," *IEEE Transactions on Industrial Electronics*, vol. 50, no. 4, pp. 767-776, Aug. 2003.

[8] J.E. Baggio, H.L. Hey, H. A. Grundling, H. Pinheiro and J. R. Pinheiro, "Discreate control for three-level boost pfc converter," *in Proceedings of the 24th International Telecommunications Energy Conference*, pp.627-633, 2002.

[9] J.M. Kwon, B. H. Kwon and K.H. Nam, "Three-phase photovoltaic system with three-level boosting mppt control," *IEEE Transactions on Power Electronics*, vol. 23, no. 5, pp.2319-2327, 2008.

[10] L.S. Yang, T.J. Liang and J.F. Chen, "Transformerless DC-DC converters with high step-up voltage gain," *IEEE Transactions on Industrial Electronics*, vol. 56, no.8, pp. 3144-3152, 2009.

[11] X. Ruan, B. Li, Q. Chen, S. Tan and C.K. Tse, "Fundamental considerations of three-level DC–DC converters: topologies, analyses, and control," *IEEE Transactions on Circuits and Systems*, vol. 55, no. 11, pp. 3733-3743, 2008.

[12] W. Li and X. He, "Review of non-isolated high-step-up DC/DC converters in photovoltaic grid-connected applications," *IEEE Transactions on Industrial Electronics*, vol. 58, no. 4, pp. 1239-1250, 2011.

[13] Y. Cheng, C. Qian, M.L. Crow, S. Pekarek and S. Atcitty, "A comparison of diode-clamped and cascaded multilevel converters for a STATCOM with energy storage", *IEEE Transactions on Industrial Electronics*, vol. 53, no. 5, 1512-1521, 2006.

[14] S. Laali, E. Babaei and M.B.B. Sharifian, "Reduction the number of power electronic devices of a cascaded multilevel inverter based on new general topology," *Journal of Operation and Automation in Power Engineering* ,vol. 2, no. 2, pp.

81-90, 2014.

[15] M.R. Banaei and E. Salary, "New multilevel inverter with reduction of switches and gate driver", *Energy Conversion and Management*, vol. 52, pp. 1129-1136, 2011.

[16] N.A. Rahim and J. Selvaraj, "Multistring five-level inverter with novel PWM control scheme for PV application," *IEEE Transactions on Power Electronics*, vol. 57, no. 6, pp. 2111-2123, 2010.

[17] B. Axelrod, Y. Berkovich and A. Ioinovici, "Switched-capacitor/switched-inductor struct-ures for getting transformer less hybrid DC-DC pwm converters," *IEEE Transactions on Circuits and Systems,* vol. 55, no. 2, pp.687-696, 2008.

[18] J.M. Shen, H.L. Jou, J. C. Wu and K. D. Wu, "Five-level inverter for renewable power generation system," *IEEE Transactions on Energy Conversion*, vol. 28, no. 2, pp. 257-266, 2013.

[19] S.R. Pulikanti, G. Konstantinou and V.G. Agelidis, "Hybrid seven-level cascaded active neutral-point-clamped-based multilevel converter under SHE-PWM," *IEEE Transactions on Industrial Electronics*, vol. 60, no. 11, pp. 4794-4804, 2013.

[20] Y. Ounejjar, K. Al-Hadded and L.A. Dessaint, "A novel six-band hysteresis control for the packed u cells seven-level converter: experimental validation," *IEEE Transactions on Industrial Electronics*, vol. 59, no. 10, pp. 3808-3816, 2012.

[21] S. Khomfoi and L.M. Tolbert, Multilevel power converters. Power electronics handbook. Elsevier; 2007, pp. 451-82 [chapter 17].

[22] K.A. Corzine, M.W. Wielebski, F.Z. Peng and J. Wang, "Control of cascaded multi-level inverters," *IEEE Transactions on Power Electronics*, vol. 19, no. 3, pp. 732-738, 2004.

[23] E.A. Mahrous, N.A. Rahim, W.P. Hew and K.M. Nor, "Proposed nine switches five level inverter with low switching frequencies for linear generator applications", *in Proceedings of the Internati-onal Conference on Power Electronics and Drives Systems*, pp. 648-653, 2005.

[24] E. A. Mahrous, N.A. Rahim and W. P. Hew, "Three-phase three-level voltage source inverter with low switching frequency based on the two-level inverter topology", *IET Proceedings on Electric Power Applications*, vol. 1, Issue 4, pp. 637-641, 2007.